J Mater Sci (2015) 50:5458–5465
DOI 10.1007/s10853-015-9091-0

Ion-linked double-network hydrogel with high toughness and stiffness

Jilong Wang[1] · Junhua Wei[1] · Siheng Su[1] · Jingjing Qiu[1] · Shiren Wang[2]

Received: 20 March 2015 / Accepted: 9 May 2015 / Published online: 19 May 2015

Abstract In this paper, a facile one-pot method was developed to fabricate ion cross-linked calcium-alginate/poly(acrylamide) (PAAm) double-network hydrogels with excellent toughness and stiffness. In comparison to the sodium alginate/PAAm hybrid gel, the as-fabricated calcium-alginate/PAAm gel demonstrated superior mechanical properties. After soaking in calcium chloride ($CaCl_2$) solution, the size of the as-synthesized hybrid gel can be well controlled without observable volumetric swelling through manipulating the equilibrium between shrinkable elastic energy from ionic (Ca^{2+}) bonds and swelling osmotic energy. This material design and processing technology are promising to fabricate complicated-shaped cartilage with high geometric fidelity. After soaking in 8 wt% $CaCl_2$ solution for 2 h, compressive strength of calcium-alginate/PAAm gel was significantly improved by 92 % compared to PAAm single network hydrogel, meanwhile the size and shape of calcium-alginate/PAAm gel were nearly changed and deformed, respectively.

Electronic supplementary material The online version of this article (doi:10.1007/s10853-015-9091-0) contains supplementary material, which is available to authorized users.

✉ Jingjing Qiu
jenny.qiu@ttu.edu

✉ Shiren Wang
s.wang@tamu.edu

Jilong Wang
jilong.wang@ttu.edu

Junhua Wei
j.wei@ttu.edu

Siheng Su
siheng.su@ttu.edu

[1] Department of Mechanical Engineering, Texas Tech University, 2500 Broadway, P.O. Box 43061, Lubbock, TX 79409, USA

[2] Department of Materials Science and Engineering, Texas A&M University, 3131 TAMU, College Station, TX 77843-3131, USA

Introduction

The natural cartilages in the human body play a crucial role in the normal joint functions involving reduction of friction, distribution of loads, and absorption of impact energy [1–3]. Traditional techniques to repair cartilage lesions, including micro-fracture technique, periosteal graft, and meniscal graft, provide temporary replacement before degradation and regrowth of cartilage. However, the regenerated cartilage is structurally, chemically, and mechanically inferior to the intact natural cartilage and results in repetitive damages [4–7]. Artificial cartilage has received tremendous interests as a candidate material to repair cartilage defects or even replace the damaged cartilage due to its easy implantation, good mechanical properties, and excellent biocompatibility without stimulating donor site morbidity [4].

Hydrogels are three-dimensional networks composed of high-molecular weight polymer, water, and cross-linker [8–10]. Due to the existence of hydrophilic polymer network, hydrogels can swell several times from dry volume under different environmental stimuli such as temperature [11], light [12], pH [13], and ionic concentration [14]. Therefore, hydrogels are widely used as drug delivery carriers [15] and superabsorbent materials [16]. However, the poor geometry fidelity and the limited mechanical properties of single network (SN) hydrogels have limited their further

biomedical applications as artificial cartilage [17, 18], muscle, and vascular [19–21]. For instance, polyvinyl-alcohol (PVA) hydrogels-based artificial cartilage did not pass clinical tests owing to their insufficiency in the strength, toughness, and friction properties [22, 23].

Recently, tremendous efforts have been devoted to improving mechanical performance of hydrogels. Composite hydrogels, which are hydrogels with fillers, are widely studied for their improved mechanical properties. However, it is generally considered that the organic/inorganic fillers, such as carbon nanotubes, clay, fibers, celluloses, and graphene oxide, may limit the biocompatibility of hydrogels [24–36]. Other chemical and physical methods to achieve tough hydrogels include complicated synthesis of precursors or cross-linkers. For instance, slide-ring hydrogels count on the design and synthesis of specific cross-linking points [37, 38]. Tetra-arm hydrogels desire homogeneous distribution of cross-linking points and chain lengths between cross-linking points [39, 40]. Hydrophobic groups-modified hydrogels depend on special functionalized precursors [41, 42]. Macromolecular microsphere composite (MMC) hydrogels employ peroxidized macromolecular microspheres as polyfunctional initiating and cross-linking centers [43–45]. All the above-mentioned methods involve complicated synthesis procedures and are usually time-consuming. Compared to those methods, double-network hydrogels attract dramatic attention since improved mechanical properties can be easily achieved by tuning inter/intramolecular interactions and structures within and between two networks using a wide variety of polymeric monomers, cross-linkers, and cross-linking methods [46–51].

Zheng and coworker reported a facile one-pot method to fabricate Agar/polyacrylamide (PAAm) double-network gel with high mechanical properties [9]. However, the harsh condition (soluble temperature 85–95 °C) to dissolve agar limited the simple manufacturing process. Sodium alginate (SA), an anionic polymer, has received increasing attention recently due to its biocompatibility, hydrophilicity, and biodegradability under normal physiological conditions, which has been widely used as an instant gel for bone tissue engineering [52].

Although the calcium-alginate/PAAm (CA/PAAm) has been developed in the recent years with remarkable tensile strength and excellent biocompatibility [24, 44, 47, 53], its applications are also limited by its shape fidelity owing to swelling. Mooney's group prepared CA/PAAm DN hydrogels with calcium sulfate ($CaSO_4$) to form ionic cross-linked Ca-alginate as the first network and then polymerized PAAm as the second network. However, the synthesized CA/PAAm exhibited low mechanical properties because the low solubility of $CaSO_4$ led to low Ca^{2+} concentration in DN hydrogels. Moreover, the poor dispersion of Ca^{2+} in thick SA solution resulted in heterogeneous cross-links. The quick response of Ca-alginate made it difficult to control the fabrication process [8, 47]. Suo and Vlassak's group improved the previous method by employing an additional step of soaking hydrogels in Ca^{2+} solution [53]. Zhou and Chen employed different ionic alginates to improve the mechanical properties [44]. Although the mechanical properties of CA/PAAm was dramatically increased, significant volumetric swelling in ionic solution soaking still existed due to the osmotic pressure, which extremely weakens the mechanical toughness and results in poor dimension and shape fidelity [40].

In this paper, robust CA/PAAm hydrogel with high dimension and shape fidelity will be achieved through swelling control with the aid of ion-sensitive segments. The ion-sensitive segments confined the double-network polymer due to ionic interactions. The schematic illustration for the synthesis of CA/PAAm DN gel is shown in Scheme 1. A one-pot method was designed to fabricate CA/PAAm DN hydrogel. Firstly, PAAm network is formed under gentle heat condition. Then the sodium alginate/PAAm (SA/PAAm) hydrogel was soaked in the $CaCl_2$ solution with a controlled concentration. The guluronic acid (G unit) blocks in different alginate chains are connected to form ionic cross-links to build second network in hydrogels through Ca^{2+}. Due to the balance between shrinkage of SA and swelling of PAAm in $CaCl_2$ solution, no obvious swelling was observed during the formation of the CA/PAAm DN hydrogel. Further studies demonstrate that this hydrogel processing strategy can be successfully used to manufacture artificial meniscus with good dimension and shape fidelity, as well as high toughness and stiffness.

Materials and methods

Materials

Acrylamide (AAm), *N*,*N*′-methylenebis (acrylamide) (MBAA), calcium chloride ($CaCl_2$), and ammonium persulfate (APS) were purchased from Sigma Aldrich. SA was kindly obtained from FMC Bio Polymer.

Synthesis of double-network hydrogel (DN)

The SA/PAAm double-network hydrogel was firstly synthesized by a novel two-step method before the synthesis of CA/PAAm. Briefly, 200 mg of SA was dissolved in 10 mL of DI water under continuous gentle stirring overnight. Then 1200 mg of AAm was dispersed into the thick SA solution before bubbling with Nitrogen for 10 min. The mixture was subsequently mixed with MBAA and APS under gentle stirring. The weight of MBAA and APS was

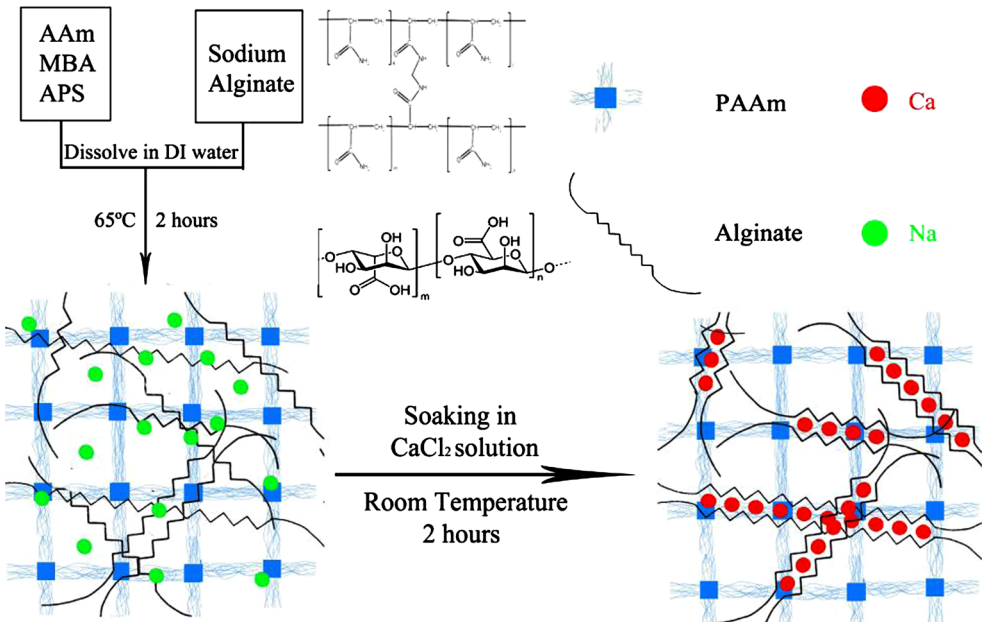

Scheme 1 Scheme of CA/PAAm double-network hydrogel

0.0025 and 0.03 times that of AAm, respectively. After 30-min stirring, the thick solution stood for 1 h to remove the bubbles. Then the transparent solution was injected into a closed Teflon mold covered with a glass slide. The mold was transferred to a glove box filled with nitrogen gas and the SA/PAAm hydrogel was prepared after 2 h of heating at 65 °C in an oil bath. After that, the pre-prepared gel was immersed in $CaCl_2$ solution to achieve CA/PAAm DN gels with higher toughness and stiffness. The SA/PAAm control sample was prepared in the same procedure without the post-processing of SA. The CA/PAAm DN gels with different concentrations of AAm and SA were manufactured in the same process and compared.

Material characterizations

The uniaxial compressive resistance properties of the hydrogels were tested on a SHIMADZU precision universal tester (AGS-X). Cylindrical gel samples were used for compression tests. The compressive strain was estimated as h/h_0, where h is the deformed height and h_0 is the original height. The compressive stress was measured as F/A_0, where F is the force applied on the gel and A_0 is the original cross section area of gel sample. The compressive rate was 1 mm min^{-1}.

Results and discussions

PAAm SN gels exhibited poor shapeability and weak mechanical properties [9]. As shown in Fig. 1, the PAAm SN hydrogels were loosely cross-linked and could not retain its shape after removal from the mold. After compression, the meniscus shape of PAAm SN gel collapsed. After soaking of SA/PAAm DN gel in 10 wt% $CaCl_2$ solution for 2 h, the meniscus shape of CA/PAAm DN hydrogel is well maintained without observable swelling, as shown in Fig. 2a. The Fig. 2b and c presented that CA/PAAm DN gel cartilage processed good geometric consistency with the tibia joint simulator. In addition, the CA/PAAm DN gel artificial meniscus demonstrated good resiliency and high shape retention without any obvious damage even after compression, stretching, and bending (as shown in Fig. 3). The easy processability, excellent compressive resistance, and good geometry fidelity make the CA/PAAm DN gel a good candidate to be applied as artificial cartilage.

The size change of the as-prepared gels in $CaCl_2$ solution at 25 °C was further studied as a function of Ca^{2+} concentration and time. Hydrogels in cylinder shape were achieved simply by mixing aqueous solutions of the polymer units, and the resultant hydrogels contain a high amount of water (73–83 %) in the CA/PAAm DN hydrogel. As shown in Fig. 4, the diameter of as-prepared hydrogel is 15.83 mm, the diameter increased after soaking 2 h in low concentration of $CaCl_2$ solution, which is due to the collapse of polymer network when the equilibrium between osmotic and elastic energies is inevitably lost [40]. However, with the increasing of Ca^{2+} concentration, the diameter of CA/PAAm DN hydrogel reduced. When the Ca^{2+} concentration is 10 wt%, the diameter of CA/PAAm DN hydrogel hardly changed, which was illustrated in the subset photo in Fig. 4.

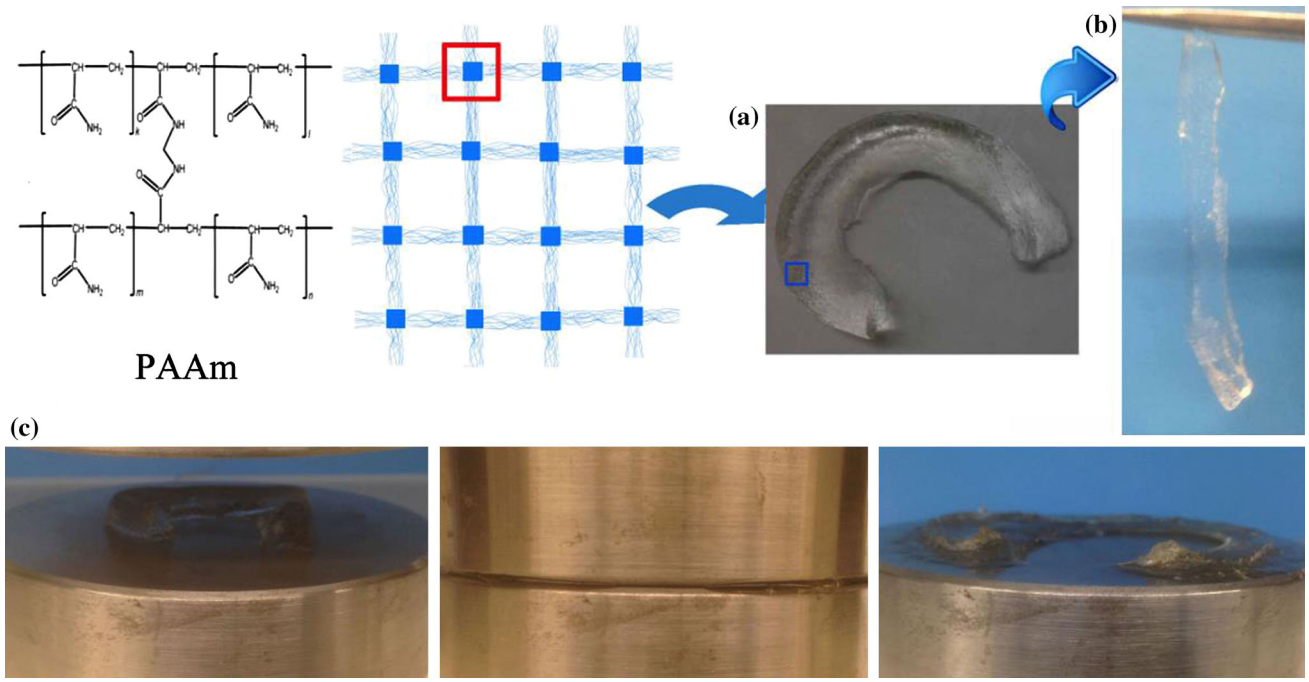

Fig. 1 Weak mechanical and free-shapeable properties of PAAm SN hydrogels **a** meniscus; **b** suspension of meniscus; **c** compression of meniscus

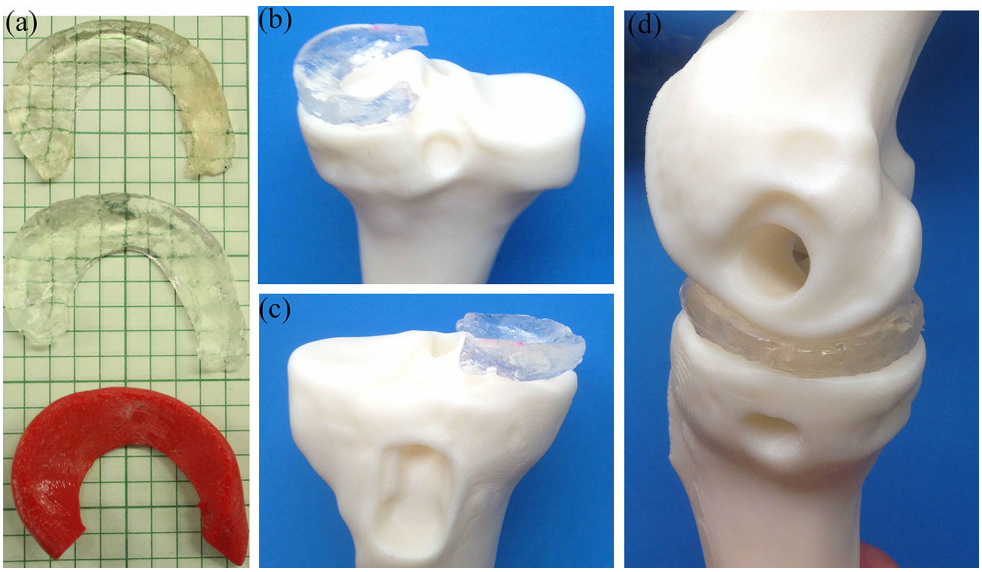

Fig. 2 **a** Comparison of the SA/PAAm gel- (*upper*) and CA/PAAm DN gel- (*middle*) based artificial cartilage and the thermoplastic acrylonitrile butadiene styrene (ABS)- based cartilage geometric model (*bottom*, dyed in *red*); **b**, **c**, and **d** are the photographs of the gel cartilage with good geometric consistency with the tibia joint simulator (Color figure online)

Two types of cross-linked polymer networks were present in CA/PAAm DN hydrogels: ion (Ca^{2+}) cross-linked alginate as the second network and covalently cross-linked PAAm as the first network. These two types of cross-linked polymers are intertwined to form interpenetrated polymer network (IPN) with toughness and stiffness similar with those of natural cartilage. The hydrogel did not demonstrate regular volumetric swelling due to the ion-responsive shrinking behavior, which was achieved through balancing swelling osmotic energy and shrinkable elastic energy from CA gel. Furthermore, the size change versus time in $CaCl_2$ with different concentrations was observed, as shown in Fig. 5. At first, in the high concentration (10 wt%) of Ca^{2+} solution, the diameter decreased

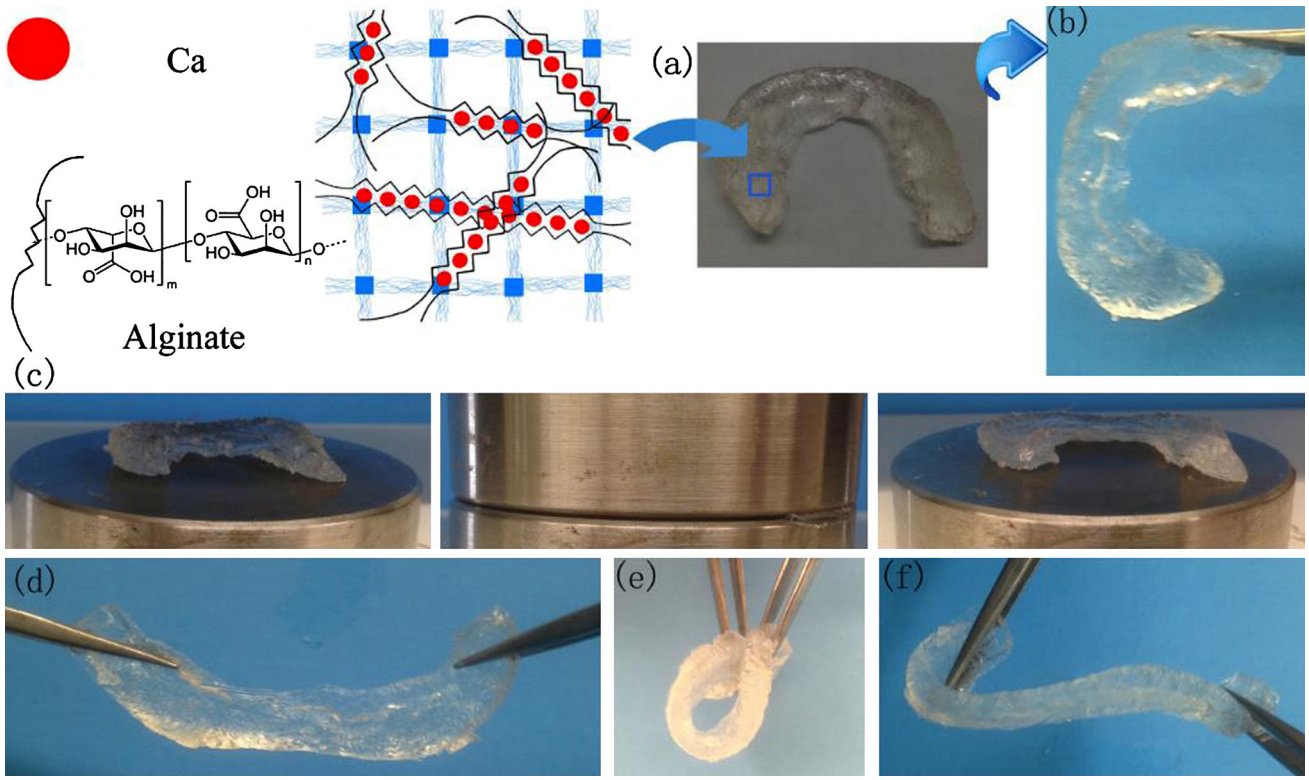

Fig. 3 Extraordinary mechanical and free-shapeable of Ca-alginate/PAAm DN hydrogels **a** meniscus; **b** suspension of meniscus; **c** compression of meniscus; **d** stretching of meniscus; **e** and **f** bending of meniscus

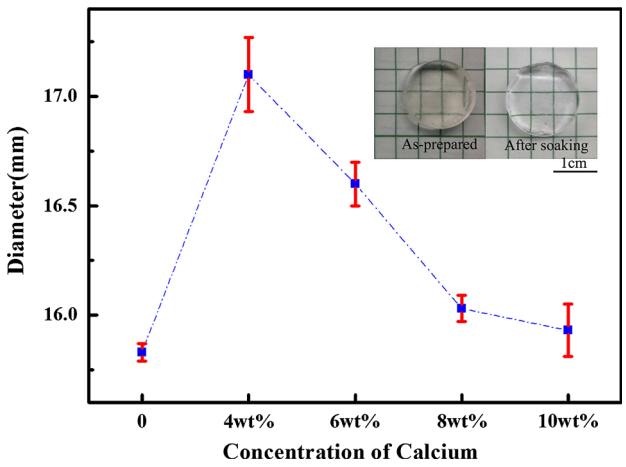

Fig. 4 Size change of hydrogel in $CaCl_2$ solution with different concentrations. Insert is photograph of hydrogel before and after soaking 10 wt% $CaCl_2$ solution for 2 h. The concentration of alginate was 20 mg mL^{-1} and AAm was 120 mg mL^{-1}

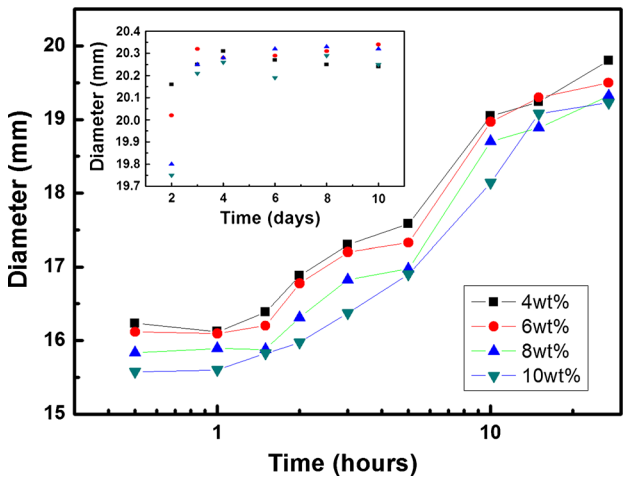

Fig. 5 Size change of hydrogel versus time in $CaCl_2$ solution with different concentrations. The concentration of alginate was 20 mg mL^{-1} and AAm was 120 mg mL^{-1}

in a small range, which resulted from the high ionically cross-linked bond. With time increasing, the diameter increased gradually due to osmotic swelling. After that, the equilibrium was crushed owing to the shrinkable elastic energy and was weakened since ionic cross-linked network was completely built. In this period, the diameter increased dramatically. Finally, the size of DN hydrogel in different Ca^{2+} concentrations was kept in a same range, which demonstrated that a new balance between the osmotic energy and elastic energy was obtained when the network was stretched after swelling.

In addition, the diameter change with different ratios of alginate and PAAm was showed in Fig. S1. With the

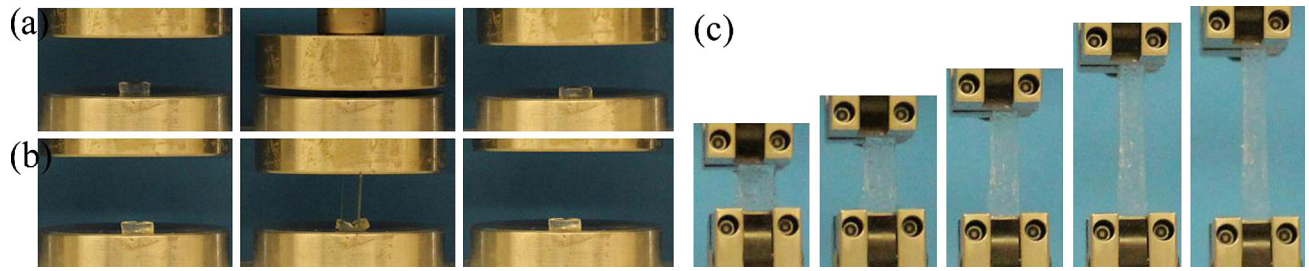

Fig. 6 Mechanical tests of CA/PAAm DN gels with high PAAm concentration indicated **a** good resiliency; **b** excellent slicing resistance; and **c** good elasticity

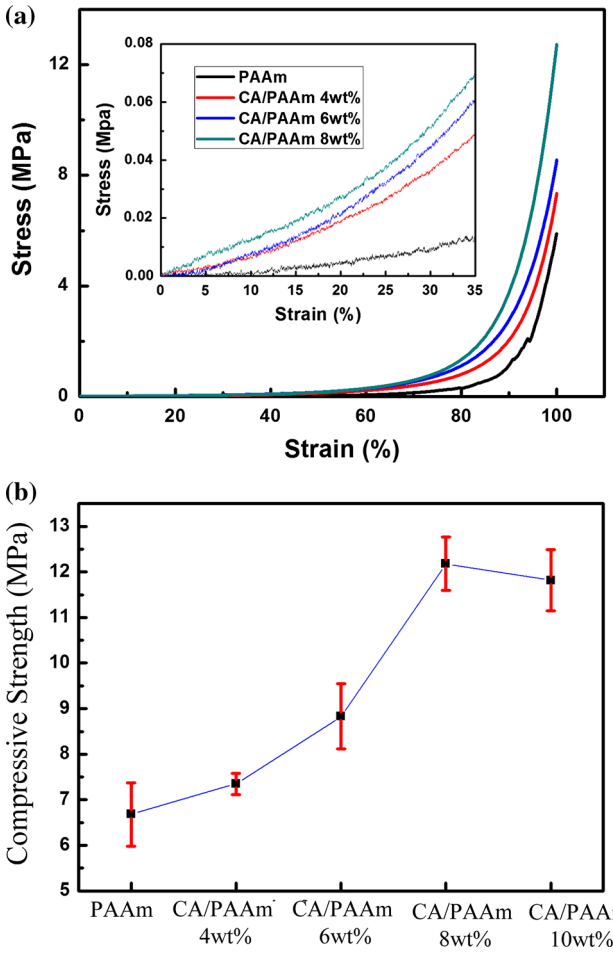

Fig. 7 Comparison of the uniaxial compression properties of CA/PAAm DN gel after soaked in different concentrations of Ca^{2+}, the concentration of Na-alginate was specified to be 20 mg mL^{-1} and AAm was 120 mg mL^{-1}. **a** Compressive stress–strain curves of CA/PAAm DN gel; **b** comparison of maximum compressive stress with different concentrations of Ca^{2+}

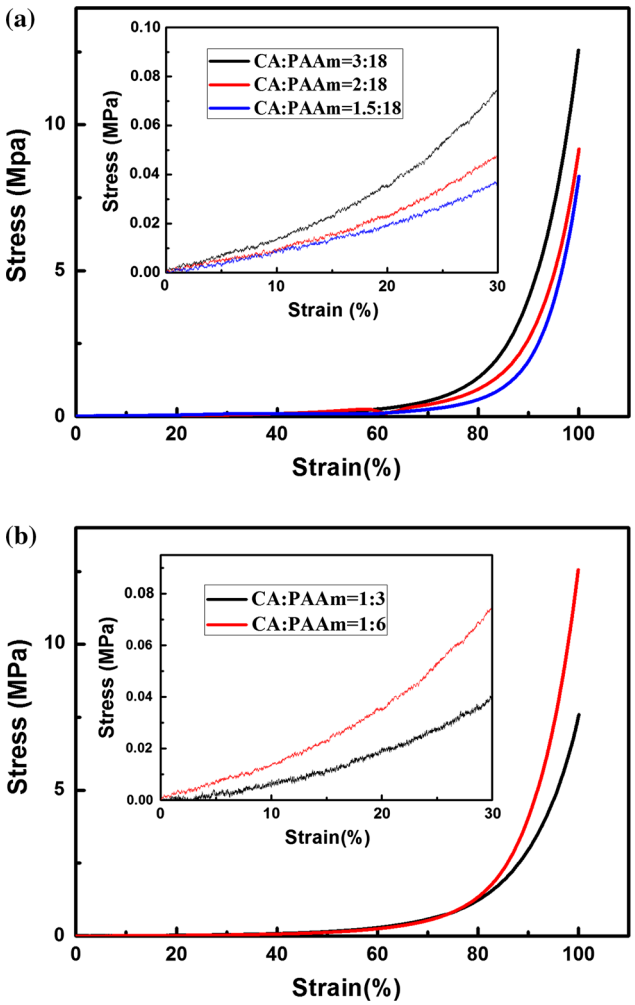

Fig. 8 **a** Comparison of the compressive properties of CA/PAAm DN gel with different alginate concentrations. The concentration of AAm (120 mg mL^{-1}) was specified; **b** comparison of the compression properties of CA/PAAm DN gel with different AAm concentrations. The concentration of alginate (20 mg mL^{-1}) was specified. The concentration of $CaCl_2$ solution is 10 wt% for the preparation of all those gels

increment of alginate ratio, the diameter of DN hydrogel decreased since the shrinkable energy from Ca^{2+} ionic bonds overcame the osmotic swelling. However, the size of DN gel became smaller with the reduction in PAAm ratio, because the equilibrium of osmotic and elastic energy was broken.

Furthermore, the superior mechanical properties of CA/PAAm DN hydrogel were showed in the Fig. 6 with excellent resiliency, slicing resistance, and elasticity.

Most importantly, the DN gel in cylinder and film both processed the ability to restore rapidly to their original shape upon removal of the external compression or tension.

The uniaxial compressive strength of the CA/PAAm DN was comprehensively studied. The compressive property of DN gel samples as a function of different Ca^{2+} concentrations was compared in Fig. 7. The as-prepared SA/PAAm hydrogels were immersed into solutions with different concentrations of $CaCl_2$. With the increment of Ca^{2+} concentration from 2 to 10 wt%, the compressive strength was enhanced by increased Ca^{2+} concentration, which demonstrated that the guluronic acid (G unit) in different alginate chains form ionic cross-links though calcium divalent cations, resulting in a CA network [8]. When the Ca^{2+} concentration was higher than 8 wt%, the compressive strength indicated no obvious variation, which demonstrated that the equilibrium of Ca^{2+} ion cross-linked alginate was achieved. The compressive modulus of DN gels was also enhanced with the increment of Ca^{2+} concentration (As shown in inset of Fig. 7a).

As shown in Fig. 8, different ratios between alginate and acrylamide were studied to reveal the effects of composition on the mechanical properties of the as-fabricated DN gels. As shown in Fig. 8a, when the content of AAm is specified in DN hydrogels, with the increasing content of alginate, the compressive strength and modulus increased simultaneously. Figure 8b indicated that the increment of AAm content also led to the improvement of compressive strength and modulus with set content of alginate. These indicated that the improvement of compressive strength and modulus was derived from the combination of PAAm and CA network [8].

Conclusions

In conclusion, a facile one-pot synthesis is developed to fabricate ion-linked Ca-alginate/PAAm double-network hydrogels. In this paper, AAm is first to be polymerized before the ion cross-linking of alginate. The swelling behavior of this ion-responsive double-network gel can be precisely controlled when the ion concentration is 8 wt%. This double-network hydrogel is promising to be fabricated into complex-shaped artificial cartilage with superior geometric fidelity, excellent compressive resistance, good resiliency, and elasticity that is comparable to the native cartilage. This research may open a pathway of biomedical applications for composite hydrogels.

Acknowledgements The authors would like to acknowledge the support from NSF Grant #1228127.

References

1. Arakaki K, Kitamura N, Fujiki H et al (2010) Artificial cartilage made from a novel double-network hydrogel: in vivo effects on the normal cartilage and ex vivo evaluation of the friction property. J Biomed Mater Res A 93:1160–1168
2. Ateshian GA (2007) Artificial cartilage: weaving in three dimensions. Nat Mater 6:89–90
3. Freed LE, Engelmayr GC, Borenstein JT, Moutos FT, Guilak F (2009) Advanced material strategies for tissue engineering scaffolds. Adv Mater 21:3410–3418
4. Fukuda A, Kato K, Hasegawa M et al (2005) Enhanced repair of large osteochondral defects using a combination of artificial cartilage and basic fibroblast growth factor. Biomaterials 26:4301–4308
5. Steadman J, Rodkey W, Briggs K, Rodrigo J (1999) The microfracture technic in the management of complete cartilage defects in the knee joint. Der Orthop 28:26–32
6. Ochi M, Sumen Y, Jitsuiki J, Ikuta Y (1995) Allogeneic deep frozen meniscal graft for repair of osteochondral defects in the knee joint. Arch Orthop Trauma Surg 114:260–266
7. Shahgaldi B, Amis A, Heatley F, McDowell J, Bentley G (1991) Repair of cartilage lesions using biological implants. A comparative histological and biomechanical study in goats. J Bone Jt Surg Br 73:57–64
8. Sun J-Y, Zhao X, Illeperuma WR et al (2012) Highly stretchable and tough hydrogels. Nature 489:133–136
9. Chen Q, Zhu L, Zhao C, Wang Q, Zheng J (2013) A robust, one-pot synthesis of highly mechanical and recoverable double network hydrogels using thermoreversible sol-gel polysaccharide. Adv Mater 25:4171–4176
10. Wang J, Qiu J, Wang S (2013) 3D Core-shell simulation of hydrogel swelling behavior for controlled drug delivery. In: ASME 2013 International Mechanical Engineering Congress and Exposition. doi:10.1115/IMECE2013-65070
11. Meid J, Dierkes F, Cui J et al (2012) Mechanical properties of temperature sensitive microgel/polyacrylamide composite hydrogels—from soft to hard fillers. Soft Matter 8:4254–4263
12. Charati MB, Lee I, Hribar KC, Burdick JA (2010) Light-sensitive polypeptide hydrogel and nanorod composites. Small 6:1608–1611
13. Bai H, Li C, Wang X, Shi G (2010) A pH-sensitive graphene oxide composite hydrogel. Chem Commun 46:2376–2378
14. Garg T, Singh S, Goyal AK (2013) Stimuli-sensitive hydrogels: an excellent carrier for drug and cell delivery. Crit Rev Ther Drug 30:369–409
15. Altunbas A, Lee SJ, Rajasekaran SA, Schneider JP, Pochan DJ (2011) Encapsulation of curcumin in self-assembling peptide hydrogels as injectable drug delivery vehicles. Biomaterials 32:5906–5914
16. Bao Y, Ma J, Li N (2011) Synthesis and swelling behaviors of sodium carboxymethyl cellulose-g-poly (AA-co-AM-co-AMPS)/MMT superabsorbent hydrogel. Carbohydr Polym 84:76–82
17. Huey DJ, Hu JC, Athanasiou KA (2012) Unlike bone, cartilage regeneration remains elusive. Science 338:917–921
18. Chen T, Buckley M, Cohen I, Bonassar L, Awad HA (2012) Insights into interstitial flow, shear stress, and mass transport effects on ECM heterogeneity in bioreactor-cultivated engineered cartilage hydrogels. Biomech Model Mechanobiol 11:689–702
19. Lee H, Xia CG, Fang NX (2010) First jump of microgel; actuation speed enhancement by elastic instability. Soft Matter 6:4342–4345
20. Keplinger C, Sun JY, Foo CC, Rothemund P, Whitesides GM, Suo ZG (2013) Stretchable, transparent, ionic conductors. Science 341:984–987
21. Shepherd RF, Ilievski F, Choi W et al (2011) Multigait soft robot. Proc Natl Acad Sci USA 108:20400–20403

22. Kobayashi M, Oka M (2004) Composite device for attachment of polyvinyl alcohol-hydrogel to underlying bone. Artif Organs 28:734–738
23. Kobayashi M, Oka M (2004) Characterization of a polyvinyl alcohol-hydrogel artificial articular cartilage prepared by injection molding. J Biomater Sci Polym Ed 15:741–751
24. Fan J, Shi Z, Lian M, Li H, Yin J (2013) Mechanically strong graphene oxide/sodium alginate/polyacrylamide nanocomposite hydrogel with improved dye adsorption capacity. J Mater Chem A 1:7433–7443
25. Servant A, Methven L, Williams RP, Kostarelos K (2013) Electroresponsive polymer–carbon nanotube hydrogel hybrids for pulsatile drug delivery in vivo. Adv Healthc Mater 2:806–811
26. Shin SR, Jung SM, Zalabany M et al (2013) Carbon-nanotube-embedded hydrogel sheets for engineering cardiac constructs and bioactuators. ACS Nano 7:2369–2380
27. Yi J-Z, Zhang L-M (2008) Removal of methylene blue dye from aqueous solution by adsorption onto sodium humate/polyacrylamide/clay hybrid hydrogels. Bioresour Technol 99:2182–2186
28. Cong HP, Wang P, Yu SH (2014) Highly elastic and superstretchable graphene oxide/polyacrylamide hydrogels. Small 10:448–453
29. Yu S, Li N, Higgins D et al (2014) Self-assembled reduced graphene oxide/polyacrylamide conductive composite films. ACS Appl Mater 6:19783–19790
30. Song W, Wang X, Wang Q, Shao D, Wang X (2015) Plasma-induced grafting of polyacrylamide on graphene oxide nanosheets for simultaneous removal of radionuclides. Phys Chem Chem Phys 17:398–406
31. Wang Q, Cai J, Zhang L et al (2013) A bioplastic with high strength constructed from a cellulose hydrogel by changing the aggregated structure. J Mater Chem A 1:6678–6686
32. Wang JL, Wei JH, Su SH, Qiu JJ (2015) Novel fluorescence resonance energy transfer optical sensors for vitamin B-12 detection using thermally reduced carbon dots. New J Chem 39:501–507
33. Wang J, Zhou Z, Huang X et al (2013) Effect of alcohol pretreatment in conjunction with atmospheric pressure plasmas on hydrophobizing ramie fiber surfaces. J Adhes Sci Technol 27:1278–1288
34. Zhou Z, Liu XC, Hu BT et al (2011) Hydrophobic surface modification of ramie fibers with ethanol pretreatment and atmospheric pressure plasma treatment. Surf Coat Technol 205:4205–4210
35. Wang J, Su S, Wei J et al (2015) Ratio-metric sensor to detect riboflavin via fluorescence resonance energy transfer with ultra-high sensitivity. Phys E 72:17–24
36. Wang J, Qiu J (2015) Luminescent graphene quantum dots: as emerging fluorescent materials for biological application. Sci Adv Mater. doi:10.1166/sam.2014.2035
37. Murayama H, Imran AB, Nagano S et al (2008) Chromic slide-ring gel based on reflection from photonic bandgap. Macromolecules 41:1808–1814
38. Bin Imran A, Esaki K, Gotoh H et al (2014) Extremely stretchable thermosensitive hydrogels by introducing slide-ring polyrotaxane cross-linkers and ionic groups into the polymer network. Nat Commun 5:5124–5132
39. Matsunaga T, Sakai T, Akagi Y, U-i C, Shibayama M (2009) Structure characterization of tetra-PEG gel by small-angle neutron scattering. Macromolecules 42:1344–1351
40. Kamata H, Akagi Y, Kayasuga-Kariya Y, Chung U, Sakai T (2014) "Nonswellable" hydrogel without mechanical hysteresis. Science 343:873–875
41. Stile RA, Healy KE (2001) Thermo-responsive peptide-modified hydrogels for tissue regeneration. Biomacromolecules 2:185–194
42. Appel EA, Tibbitt MW, Webber MJ, Mattix BA, Veiseh O, Langer R (2015) Self-assembled hydrogels utilizing polymer-nanoparticle interactions. Nat Commun 6:6295. doi:10.1038/ncomms7295
43. Zhai D, Zhang H (2013) Investigation on the application of the TDGL equation in macromolecular microsphere composite hydrogel. Soft Matter 9:820–825
44. Zhao J, Jiao K, Yang J, He C, Wang H (2013) Mechanically strong and thermosensitive macromolecular microsphere composite poly (*N*-isopropylacrylamide) hydrogels. Polymer 54:1596–1602
45. Jiang FZ, Huang T, He CC, Brown HR, Wang HL (2013) Interactions affecting the mechanical properties of macromolecular microsphere composite hydrogels. J Phys Chem B 117: 13679–13687
46. Yang CH, Wang MX, Haider H et al (2013) Strengthening alginate/polyacrylamide hydrogels using various multivalent cations. ACS Appl Mater 5:10418–10422
47. Darnell MC, Sun JY, Mehta M et al (2013) Performance and biocompatibility of extremely tough alginate/polyacrylamide hydrogels. Biomaterials 34:8042–8048
48. Naficy S, Razal JM, Whitten PG, Wallace GG, Spinks GM (2012) A pH-sensitive, strong double-network hydrogel: poly (ethylene glycol) methyl ether methacrylates–poly (acrylic acid). J Polym Sci Polym Phys 50:423–430
49. Kitamura N, Kurokawa T, Fukui T, Gong JP, Yasuda K (2014) Hyaluronic acid enhances the effect of the PAMPS/PDMAAm double-network hydrogel on chondrogenic differentiation of ATDC5 cells. BMC Musculoskelet Disord 15:222–228
50. Jang SS, Goddard WA, Kalani MYS (2007) Mechanical and transport properties of the poly (ethylene oxide)-poly (acrylic acid) double network hydrogel from molecular dynamic simulations. J Phys Chem B 111:1729–1737
51. Yasuda K, Ping Gong J, Katsuyama Y et al (2005) Biomechanical properties of high-toughness double network hydrogels. Biomaterials 26:4468–4475
52. Li ZS, Ramay HR, Hauch KD, Xiao DM, Zhang MQ (2005) Chitosan–alginate hybrid scaffolds for bone tissue engineering. Biomaterials 26:3919–3928
53. Li JY, Illeperuma WBK, Suo ZG, Vlassak JJ (2014) Hybrid hydrogels with extremely high stiffness and toughness. ACS Macro Lett 3:520–523